

Exploring polyhedral mesh generation from Delaunay tetrahedral meshes

Sergio Salinas*

Magdalena Alvarez†

Nancy Hitschfeld‡

Abstract

In this paper we propose a new algorithm to generate polyhedral meshes based on the concept of terminal-face regions. Terminal face-regions are built from the union of tetrahedra by a face that fulfill some joining criterion. For this, we introduce first the concept of terminal-face region and how it can be seen as a natural extension of 2D terminal-edge regions [20]. Next, we include the related work in 3D polyhedral mesh generation and then the algorithm we have designed and implemented to generate polyhedral meshes. Finally, we present statistics about the kind of generated polyhedral meshes, and also a theoretical comparison with Voronoi meshes.

1 Introduction

Going from flat (2D) meshes to 3D shapes (volumetric meshes) is a big step in computer science and engineering simulations. Volumetric meshing divides a 3D object into tiny pieces to exactly represent its volume, which is important for running simulations. Mesh generation methods are important in science, engineering, and computer graphics. Tetrahedral meshes [33, 21, 7, 22, 12] and hexahedral meshes [18, 8] are chosen based on the problem and the used numerical method. In addition, there are approaches to generate mixed element meshes [31, 11] and polygonal and polyhedral meshes [1, 9, 27, 32, 6, 23], with polygonal/polyhedral cells as Voronoi regions too. Mesh generation algorithms can be divided into direct and indirect algorithms [16], with the latter having the advantage of using robust open source for initial meshes, like Tetgen [22], Tetwild [12], and CGAL [2].

With respect to the numerical methods, the Finite Element Method (FEM) has been expanded to include general polyhedral cells, and a new method called the Virtual Element Method (VEM) has been created for 2D and 3D problems. Research is now ongoing to improve and evaluate the VEM in different applications [4, 25, 24, 26]. VEM has been already applied in various fields, including solid mechanics [5, 30, 29], fluid dynamics [28], and modeling of brittle crack prop-

agation [13].

In water flow simulations of large areas, unstructured grids are needed. A tool called MODFLOW-USG [17] can handle different mesh setups. It uses a Control Volume Finite Difference (CVFD) approach, requiring a line connecting the centers of two adjacent cells to intersect the mutual boundary perpendicularly. This mirrors earlier efforts in simulating semiconductor devices with polyhedral Delaunay meshes with Voronoi regions as control volumes [10, 11].

Due to the requirements to count with polyhedral mesh generators that allow researchers to evaluate how general polyhedral cells can be and still give accurate simulation results, we present a first attempt to study the kind of polyhedra that can be generated by joining tetrahedra from a tetrahedral mesh. We present an algorithm and describe the properties of the built polyhedral cells. The preliminary experimental evaluation shows that the generated polyhedra are very far from convex cells and need to be further study too see if these kind of cells are useful and provide some advantages in the context of some specific simulation in comparison to Voronoi cells. A mesh composed of proper non-convex polyhedral cells should require less cells and points to model complex geometries than meshes composed of convex cells. Currently, together with a good point distribution, the strongest requirement for the VEM cells seems to be that polyhedron kernels should not be empty [26].

2 Basic concepts

In this section we introduce the concepts needed to understand the proposed algorithm. Several concepts are lemmas and theorems presented in [19, 3, 20], but others are new concepts and definitions to handle tetrahedral meshes.

We want to extend the concept of terminal-edge region, defined in [20], to faces in 3D, and convert them to polyhedrons to generate volume meshes. One of the problem of doing this extension, is what is “the largest face of a tetrahedron”, in such a way that we can define a path of tetrahedra. There are several criteria to define which face of a tetrahedron is the largest or the smallest, we are going to call them “Joining criteria”. Given a tetrahedral mesh $\tau = (V, E, F)$, we can define:

*ssalinas@dcc.uchile.cl, DCC, Universidad de Chile, Chile.

†DCC, Universidad de Chile, Chile.

‡nancy@dcc.uchile.cl, DCC, Universidad de Chile, Chile.

DEFINITION 1. **Joining criterion** For any tetrahedron t_i , the Joining criterion is a metric used to rank the faces of t_i ordered from the largest to the smallest. There is only one largest-face, if two faces have the same size, then one of them is chosen as the largest arbitrarily.

A joining criterion can be for example the area of the face, then we can rank the faces of the tetrahedron according to which tetrahedron has the largest and the smallest face area. With this already defined, we can extend the concept of terminal edge and longest-edge propagation path [19] to faces in a tetrahedral mesh τ with a Joining criterion J :

DEFINITION 2. **Terminal-face** A face is a terminal-face f_i if two adjacent tetrahedrons t_a, t_b to f_i share their respective (common) largest-face, according to J . This means, that f_i is the largest-face of both tetrahedrons that share f_i . If $t_b = \emptyset$, then f_i is called border terminal-face.

DEFINITION 3. **Largest-face propagation path (Lfpp)** For any tetrahedron t_0 of any tetrahedralization τ , the Largest-Face Propagation Path of t_0 ($Lfpp(t_0)$) is the ordered list of all the tetrahedrons $t_0, t_1, t_2, \dots, t_{n-1}$, such that t_i is the neighbor tetrahedron of t_{i-1} by the largest face of t_{i-1} , for $i = 1, 2, \dots, n - 1$.

For a terminal-face $f_i \in \tau$, there are various Lfpps that ends in the same f_i , it is the case even when f_i is a border face, we are going to call the set of Lfpp with the same terminal face a terminal-face region.

DEFINITION 4. **Terminal-face region** A terminal-face region R is a region formed by the union of all tetrahedrons t_i such that $Lfpp(t_i)$ has the same terminal-face.

Figure 1 illustrates examples of terminal-face regions generated using the incircle criterion. Meanwhile, Figure 2 displays the largest polyhedron, derived from the same tetrahedralization, created using two different joining criteria. With the concepts defined above, we have a proper extension of the terminal-edge region to faces in tetrahedral meshes.

In order to accelerate the generation of terminal-face regions we develop a classification system for each face of τ . For each face $f_i \in \tau$, a face can be a frontier-face or internal-face.

DEFINITION 5. **Frontier-face** A frontier-face f_i is a face that is shared by two tetrahedron t_1, t_2 , each

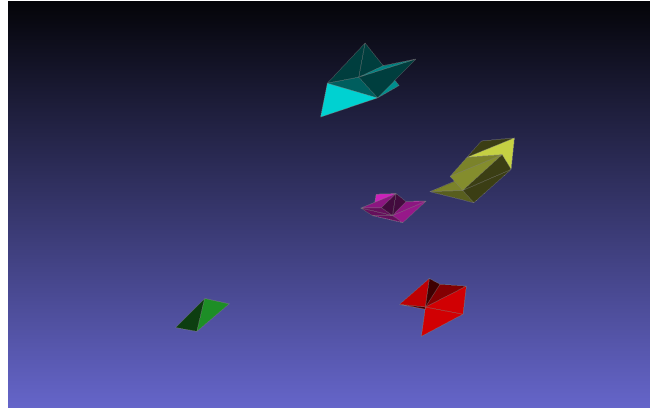


Figure 1: Example of five terminal-face region generated using the incircle joining criterion.

one belonging to a different terminal-face region, that means that f_i is not the largest-face of neither t_1 nor t_2 . If $t_2 = \emptyset$ then f_i is a frontier-face even if ef_i is a border terminal-face.

DEFINITION 6. **Internal-face** A internal-face f_i is a face that is shared by two tetrahedrons t_1, t_2 , each one belonging to a same terminal-face region. In other words, f_i is an internal-face if f_i is neither a terminal-face nor frontier-face.

For the context of this work, we only need the frontier-faces, as those faces will be faces of the polyhedral mesh at the end of the algorithm, internal-faces will be removed during the process of joining tetrahedrons. One property that terminal-face regions must obey, for their use as polyhedrons in a polyhedral mesh, is that they must not overlap.

LEMMA 2.1. Let τ be a tetrahedral mesh of any set of points P with a Joining criterion J . Then the set of terminal-face regions in τ do not overlap.

PROOF 1. By contradiction. Let us assume the tetrahedron t_k belongs to two terminal-face region R_i, R_j , each one with the terminal-faces f_i, f_j , respectively. Since t_k has only one largest-face, $Lfpp(t_k)$ has to end in either f_i or f_j , but by definition of the Joining criterion, t_k only have one largest-face, then, t_k only can have one Lfpp, thus $Lfpp(t_k)$ have to end either f_i or f_j but not both.

Hence, a tetrahedron t_k can not belong to two terminal-face regions R_i, R_j , and therefore there are not overlapping terminal-face regions in τ . ■

As in 2D, terminal-edge regions can contain frontier-edges in its interior, in 3D, terminal-face regions can contain frontier-faces in their interior. We will refer to this kind of frontier faces as barrier-faces.

DEFINITION 7. Barrier-face Given a terminal-face region R_i , any frontier-face $f \in R_i$ that is not part of the boundary δR_i is called a barrier-face.

DEFINITION 8. Barrier-edge tip A barrier tip in a terminal-face region R_i is an edge incident to only one frontier-face (particularly a barrier-face), and the rest of the faces are internal-faces.

3 Algorithm

In this section, we present our algorithm to generate polyhedral meshes. The algorithm takes as input a tetrahedral mesh $\tau = (V, E, F)$, a Joining criterion J , and return a polyhedral mesh $\tau' = (V, E', F')$. The algorithm has 3 main phases: Label phase, Traversal phase and Repair phase.

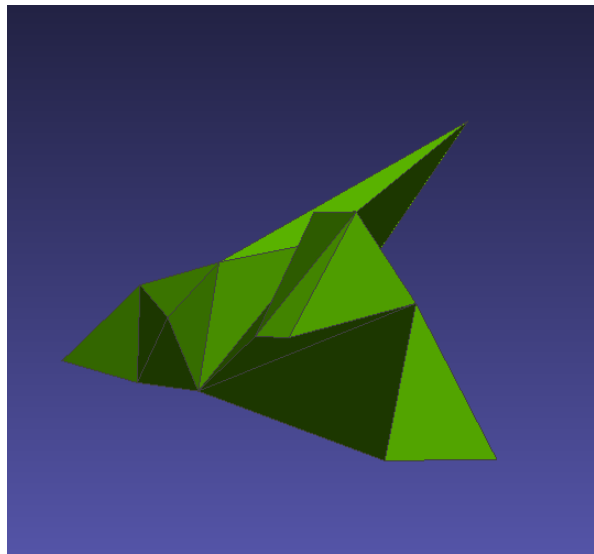
For the understanding of the algorithm, we are going to assume that we have a data structure with all geometrical information of the tetrahedral mesh. For the output we use a list of polyhedrons, and each polyhedron is represented as a list of faces.

3.1 Label phase The first step to generate the new polyhedral mesh is to define whose faces are going to be faces of the output mesh (i.e. the frontier-faces), and choose one tetrahedron t_i per terminal-face region R_i , to be used in the Traversal phase to generate the new polyhedron, we are going to name to t_i as seed tetrahedron, and it is a tetrahedron adjacent to a terminal-face. For this reason, as equal as the 2D algorithm, we first with the Label phase.

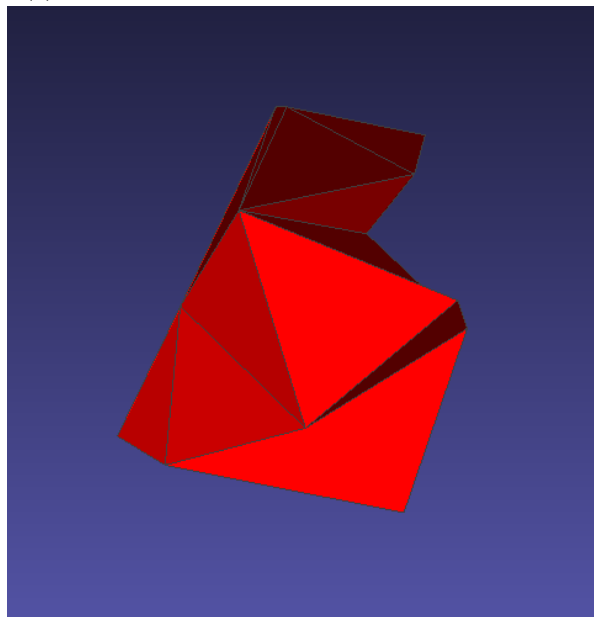
The Label phase receives $\tau = (V, E, F)$ as input, return two auxiliary arrays with information of the mesh:

- **Seed array**, of equal size to the number of tetrahedrons, with the indices of all the seed tetrahedrons in τ .
- **Frontier-face bitvectors**, of equal size to the number of faces $|F|$, in where each element i is set as true if the face f_i is a frontier-face, and false is not.

Those auxiliary arrays are equivalent to the auxiliary data structure used in the 2D algorithm for the polygonal mesh generation. Those arrays will be use in the Traversal phase and the Repair phase.



(a) Polyhedron generated with the incircle criterion



(b) Polyhedron generated with the max area criterion

Figure 2: Comparison of two polyhedra with a greater number of faces, derived from the same tetrahedralization, generated using two different joining criteria.

For this phase, we first define a join criterion J , and each face $f_i \in \tau$ is labeled according if this accomplishes J . Examples of join criteria for a tetrahedron $t_i \in \tau$ are:

- Area criterion: The largest face of t_i is the face with maximum area of t_i and the smallest face is the face with minimum area of t_i .
- In-circle radius criterion: The largest face of t_i is the face with maximum in-circle radius of t_i and the smallest face is the face with minimum in-circle radius of t_i .

Depending on the joining criterion, the properties of the polyhedral mesh will change, in the experiments section we are going to show examples of meshes with those two criteria.

This phase is shown in Algorithm 1. The algorithm first calculates the faces that accomplish the joining criterion J of each tetrahedron $t_i \in \tau$, it is shown in line 1 – 5, for each t_i , the algorithm calculates the largest face f_j according to J , and stores it in the array `largest_array`, this array has size equal to the number of tetrahedrons in the mesh, and store the index j of the face f_j in the position i , corresponding to the position of t_i in the array. For example, for a tetrahedron t_i with the area criterion, the algorithm compares the four faces of t_i and stores the index of the largest face in `largest_array`.

Afterwards, the algorithm labels the seed tetrahedrons (lines 6 – 13), those are the tetrahedrons adjacent to a terminal-face, and that are used in the traversal phase to generate the polyhedrons. For each face $f_i \in \tau$, the algorithm gets both tetrahedrons t_i, t_j and chooses one them as a seed-edge and stores it in the `seed_array`. If f_i is a border face, then it chooses only a adjacent tetrahedron as seed.

Finally, the algorithm labels the frontier-faces (lines 14 – 21), those are the faces of the final mesh τ' . For each face $f_i \in \tau$, the algorithm gets the both tetrahedrons t_i, t_j , that shares f_i , if f_i is not the largest face of neither t_i nor t_j , or if f_i is a border face, then f_i is labeled as frontier-edge (sets as true) in the `frontier_Bitvector`. This process is exemplify in Figure 3.

With the tetrahedrons and faces already labeled, the algorithm continues to the Traversal phase.

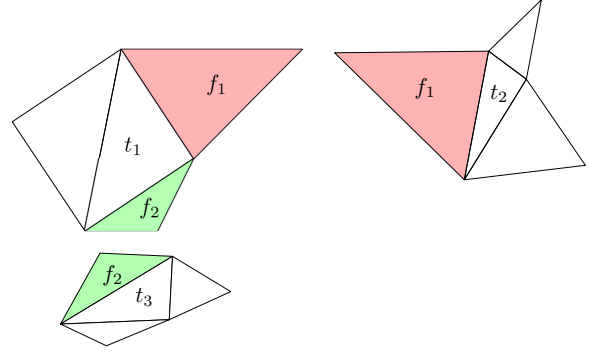


Figure 3: Example of labeling with adjacent 3 tetrahedrons, Red faces are the terminal-faces, and green faces are frontier-faces. Tetrahedron t_1 is connected to t_2 by face f_1 , and tetrahedron t_1 is connected to t_3 by face f_2 . According to the Joining criterion of the largest area, f_1 is the largest face of t_1 and t_2 , meaning that f_1 is a terminal-face, thus t_1 is chosen a seed tetrahedron. f_2 is not the largest face of t_1 and t_3 , thus f_2 is label as a frontier-face.

Algorithm 1 Label phase

Require: Tetrahedral mesh τ

Ensure: Bitvectors `frontier-face` and `max-face`, and vector `seed-list`

```

1: for all tetrahedron  $t_i$  in tetrahedron_array do  $\triangleright$ 
   Calculate largest face
2:   Calculate the join criteria  $J$  of all faces
    $f_1, f_2, f_3, f_4 \in t_i$ 
3:    $f_{max} \leftarrow \max(f_1, f_2, f_3, f_4)$ 
4:   Append  $f_{max}$  to largest_face_array
5: end for
6: for all face  $f_i$  in face_array do  $\triangleright$  Label seed
   tetrahedron
7:    $t_i, t_j \leftarrow$  adjacent tetrahedrons to  $f_i$ 
8:   if  $t_i = \emptyset$  and  $f_i$  is the largest-face of  $t_i$  then
9:     seed_face_array[ $f_i$ ] =  $t_j$ 
10:  else if  $f_i$  is the largest-face of both  $t_i$  and  $t_j$ 
   then
11:    seed_face_array[ $f_i$ ] =  $t_i$ 
12:  end if
13: end for
14: for all face  $f_i$  in face_array do  $\triangleright$  Label
   frontier-faces
15:    $t_1, t_2 \leftarrow$  adjacent tetrahedrons to  $f_i$ 
16:   if  $t_1 = \emptyset$  or  $t_2 = \emptyset$  then
17:     frontier_Bitvector[ $f_i$ ] = True
18:   else if largest_array[ $t_i$ ] is not  $f_i$  and
   largest_array[ $t_j$ ] is not  $f_i$  then
19:     frontier_Bitvector[ $f_i$ ] = True
20:   end if
21: end for

```

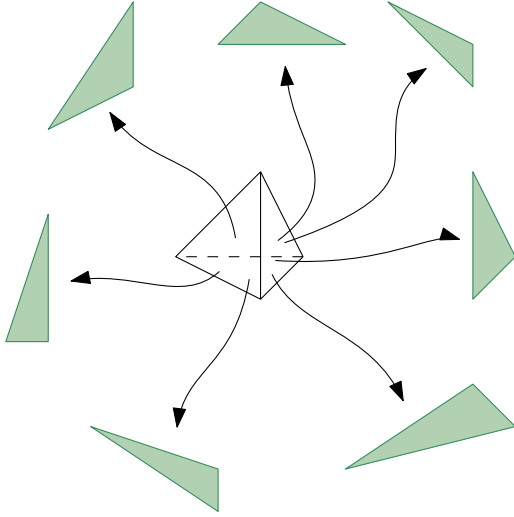


Figure 4: Visualization of the DFS, the tetrahedron at the center is a seed tetrahedron, the DFS travels inside a terminal-face region until to find a frontier-face (green faces) and stores it as a face of the new polyhedron.

3.2 Traversal phase In this phase the algorithm converts terminal-face regions into polyhedrons. To do this, for each tetrahedron $t_i \in \text{seed_array}$, the algorithm defines a polyhedron P and calls to the depth first search (DFS) algorithm [15] shown in Algorithm 2. In this DFS, the algorithm travels inside the terminal-face region using the faces of the seed tetrahedron t_i . For each tetrahedron t_j adjacent to t_i by its face, the algorithm checks if t_j contains a frontier-face f_i , if it is true, then f_i is stored in P , as part of the polyhedron, and if its is not the case, then f_i is a internal-face. Consequently, the DFS travel to the neighbors of t_j looking for others frontier-faces. This process is shown in Figure 4.

Algorithm 2 Depth First Search for polyhedron construction

Require: Seed edge e of a terminal-edge region

Ensure: Arbitrary shape polyhedron P

```

1:  $P \leftarrow \emptyset$ 
2: procedure DEPTHFIRSTSEARCH(Seed Tetrahedron  $t_i$ , Polyhedron  $P$ )
3:   Mark  $t_i$  as visited
4:   for all neighbor Tetrahedron  $t_j \in t_i$  do
5:     if common face  $f_i$  of  $t_i, t_j$  is a frontier-face
6:       then
7:         Add  $f_i$  to polyhedron  $P$ 
8:       else
9:         if  $t_j$  has not been visited yet then
10:          DepthFirstSearch( $t_j, P$ )
11:         end if
12:       end if
13:   end for
14: end procedure

```

The following Lemma demonstrates that this DFS will only travel inside a terminal-face region.

LEMMA 3.1. *Depth First Search algorithm presented in algorithm 2 only travels inside one terminal-face region R_i*

Proof Suppose that exist a terminal-face region R_j , adjacent to R_i , both connected for the frontier-face f , which is part of the tetrahedrons $t_i \in R_i$ and $t_j \in R_j$. If during the DFS the algorithm passes from R_i to R_j means that f is not labeled as a frontier-edge, but by definition, if f is the separation between R_i and R_j , then f must be a frontier-face. Thus for contradiction the DFS only travels inside one terminal-face region. \square

Notice that can occur the case that the terminal-face contains barrier-edge tips, thus, for each P generated from the DFS, the algorithm checks them. The algorithm counts the number of repeated faces in P , if there are repeated faces, it means that a face was stored two times during the DFS, indicating a barrier-face. In such cases, P is sent to the Repair phase.

3.3 Repair phase For any not simple polyhedron P_i , the algorithm uses the barrier tips to split a polyhedron in two. A barrier tips is an edge $e_i \in P_i$ that is adjacent to only one frontier-face of P_i , and the rest of faces adjacent to e_i are internal-faces. The first question to answer is how to know if edge e_i is a barrier tip.

THEOREM 3.1. *Given a terminal-edge region R_i , with F_f the set of frontier-faces of R_i , an edge e belonging to a barrier-face of R_i , and the set F_e of faces incident to e , e is a barrier tip if $|F_f| - |F_e \cap F_f| = |F_f| - 1$.*

PROOF 2. *By contradiction. Assume that e is a barrier tip and $|F_e \cap F_f| \neq 1$:*

- $|F_e \cap F_f|$ is more than 1: then there exist more than one barrier-face incident to e , but by Definition 8, e only can be incident to a barrier-face, so e is not a barrier tip.
- $|F_e \cap F_f|$ less than 1: then there is no barrier-faces (neither frontier-faces) incident to e , but by Definition 8, e have to be incident to a frontier-face. So e is not a barrier tip.

Therefore, the cardinal of $|F_e \cap F_f|$ is equal to 1, and e must fulfill that $|F_f| - |F_e \cap F_f| = |F_f| - 1$. ■

Using Theorem 3.1 we define the Algorithm 3 to get a list B_p with all the barrier tips of polyhedron P . The algorithm takes all edges e_i of the barrier-faces in P , and iterates over all them (line 2), to check if they are a barrier tip. The check is done by calculating (line 6), the formula of above, if it is true, then there is only a barrier-face adjacent to e_i , thus e_i is barrier tip.

Algorithm 3 Barrier-face Detection

Require: Polyhedron $P_i \in \tau$, F_b barrier-faces $\in P_i$

Ensure: List of barrier tips B

```

1:  $B \leftarrow \emptyset$  ▷ List of barrier tips
2: for all edges  $e_i \in F_b$  do ▷ For all the edges of the barrier-faces of  $P$ 
3:    $F_e \leftarrow$  List of all faces incident to  $e_i$ 
4:    $|F_f| \leftarrow$  number of frontier-face in  $P$ 
5:    $|F_e \cap F_f| \leftarrow$  number of faces in  $F_e$  that are also in  $F_f$ 
6:   if  $|F_f| - |F_e \cap F_f| = |F_f| - 1$  then
7:      $B \leftarrow B \cup \{e\}$  ▷  $e$  is a barrier tip
8:   end if
9: end for
10: return List of barrier tips  $B_p$ 

```

Once the algorithm has computed the set of barrier tips B , we can use them to split the polyhedron P . This split consists of converting internal-faces f_i to frontier-faces, and using the two tetrahedron adjacent to f_i as seeds to repeat the traversal phase.

This repair phase is shown in Algorithm 4. The algorithm first defines a **subseed list** L_p to store the seed tetrahedrons that will be used as seeds to generate the new polyhedra. And the **usage bitarray** A that is used as a flag to check if a seed tetrahedron has been used during the creation of a new polyhedron, thus the algorithm can avoid creating duplicate polyhedra.

Then, in line 3, the algorithm iterates over all the barrier tips $b_i \in B$. For each b_i , the algorithm selects the

barrier-face f_i incident to b_i , circles around the internal faces of b_i , and stores them in order of appearance in a sublist l . The middle internal face f_m of l is calculated. f_m is converted to a frontier-face by setting **frontier_bitvector** $[f_m] = \text{True}$. The two tetrahedron t_1 and t_2 adjacent to f_m are stored in the list L_p to be used as seed tetrahedra, and they are also marked as **True** in the **usage bitarray** A .

Later, in line 11, the algorithm constructs the polyhedron. For each tetrahedron $t_i \in L_p$, the algorithm checks if t_i has been used during the generation of a tetrahedron. If this is not the case, then the algorithm proceeds to generate a new polyhedron P' by calling the traversal phase shown in Algorithm 2. However, for each tetrahedron t_j visited in the traversal phase, $A[f_m]$ is set to **False** to avoid using t_j to generate the same polyhedron P' again. This process is repeated until there are no more seed tetrahedron in L_p , at which point all the new polyhedrons are simple polyhedrons, and are added to τ' .

Algorithm 4 Non-simple polyhedron reparation

Require: Non-simple polyhedron P , list of barrier-faces tip B

Ensure: Set of simple polyhedron S

```

1: subseed list as  $L_p$  and usage bitarray as  $A$ 
2:  $S \leftarrow \emptyset$ 
3: for all barrier-faces tip  $b_i$  in  $B$  do
4:    $f_i \leftarrow$  Barrier-face that contains  $b_i$ 
5:   Calculate the valence of  $b_i$ 
6:    $f_m \leftarrow$  middle-face incident to  $b_i$ 
7:   Label  $f_m$  as frontier-edge
8:   Save tetrahedrons  $t_1$  and  $t_2$  adjacent to  $f_m$  in  $L_p$ 
9:    $A[t_1] \leftarrow \text{True}$ ,  $A[t_2] \leftarrow \text{True}$ 
10: end for
11: for all tetrahedrons  $t_i$  in  $L_p$  do
12:   if  $A[t_i]$  is True then
13:      $A[t_i] \leftarrow \text{False}$ 
14:     Generate new polyhedron  $P'$  starting from  $t_i$  repeating the Traversal phase.
15:     Set as False all indices of tetrahedron in  $A$  used to generate  $P'$ 
16:   end if
17:    $S \leftarrow S \cup P'$ 
18: end for
19: return  $S$ 

```

Finally, τ' is a mesh composed of simple polyhedra. Notice that a more simple strategy to generate simple polyhedra is just to eliminate the barrier faces because they are internal faces and do not represent geometrical aspects to be respected from the input domain.

4 Experiments

In this section we present the preliminary results. To study the geometrical properties of the generated polyhedrons we developed a first prototype in Python. This prototype uses 4 array of structures to store the information of vertices, edges, faces and tetrahedrons of a tetrahedral mesh.

The experiments consist in testing the algorithm with 4 different kinds of tetrahedral meshes. The tetrahedral meshes are the following:

- Random meshes: We generate random points using a uniform distribution inside a cube, with method `random.rand` of python's library Numpy, and call to the method `scipy.spatial.Delaunay` in the python's library SciPy to generate Delaunay tetrahedral mesh.
- Poisson meshes: We generate random points using a Poisson distribution inside a cube, using the method `scipy.stats.qmc.PoissonDisk` of Scipy, and call to the method "Delaunay" in the python's library SciPy to generate Delaunay tetrahedral mesh.
- Quality Delaunay meshes: We call to Tetgen with the python interface of PyVista with the parameters `pqa[number]`, where `pq` generated a boundary conforming quality tetrahedral, with a maximum radius edge ratio bound as 2.0 and a minimum dihedral angle bound 0 degrees, respectively. And `a[number]` define a maximum tetrahedron volume constraint to the mesh. We define different mesh sizes by changing the value of the volume constraint `number`, the used values were 0.0008, 0.00038, 0.0000695, 0.000033, and 0.000006279, for the meshes with 496, 992, 4993, 9988 and 49999 vertices respectively.
- Grid meshes: We create equidistant points in a cube, and create a structure grid using the PyVista library, this grid is converted to a tetrahedral mesh using the method "delaunay_3d" of PyVista.

Notice that Random, Poisson and Grid meshes refers to a point distribution, but Quality meshes is a kind of mesh obtained from a mesh refinement. We used Tetgen because it is a popular mesh generator, and because the quality criteria of the tetrahedrons seems to be good intermediate between the quality of the tetrahedrons of the Poisson meshes and Grid meshes.

For each kind of mesh, we generate 5 different sizes, with 500, 1000, 5000, 10000 and 50000 vertices. We run the algorithm with two joining criteria, the in-circle criterion and the Max area criterion, it was

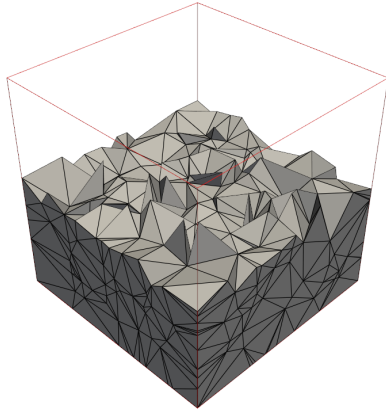
made to understand how change the behavior of the quality of the mesh with both criteria. The results are shown in Table 1, for the in-circle criterion, and the Table 2 for the Max area criterion. The tables show the number of vertices, faces, tetrahedrons and edges of the input tetrahedral mesh, the number of polyhedrons, the number of barrier-faces, the number of polyhedrons with barrier-faces, the number of polyhedrons without barrier-faces, the maximum and the average number of tetrahedrons used to create new polygons, and the time in seconds that the algorithm takes to run.

The summary of the tables can be seen in Table 3. In general, regardless of the point distribution of the meshes, the algorithm merges, on average, 3 tetrahedron per polygon, reducing the tetrahedron mesh by around 70% of the elements, and about one-fifth of the polyhedra contain barrier faces. This is even true for points not in general position, as it is the case of Grid meshes.

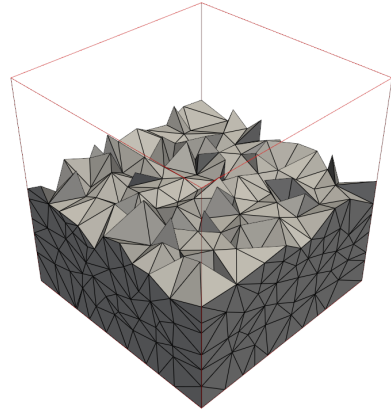
We can see differences between the two joining criterion, the in-circle criterion tends to join more tetrahedrons than the area max criterion, and the generate polyhedrons will result in less barrier-edge tips, but in they generated meshes will contains in average more tetrahedrons.

The only statistic that seems to vary depending on the distribution is the percentage of polyhedrons that remain tetrahedrons after the algorithm was applied. Poisson's meshes have the lowest percentage of tetrahedrons, while Grid meshes have the highest. However, on average, all meshes retain approximately 18.6% of their elements as tetrahedrons.

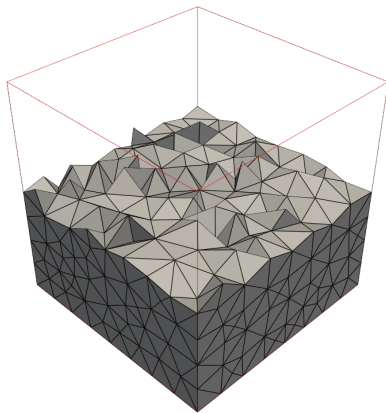
4.1 Comparison with Voronoi In order to do a simple comparison between polyhedral meshes generated by our algorithm and Voronoi meshes, we compute the number of vertices, edges, faces and polyhedra of the dual diagram of the quality tetrahedral meshes used as input shown in Table 2. Table 4 shows at the left the number of vertices, edges, faces and tetrahedra of the quality tetrahedral mesh, at the center, the same information for the Voronoi mesh and at the right for the polyhedral mesh generated by our algorithm. It can be observed that the number of vertices of the polyhedral mesh is less than in the Voronoi mesh, the number of Voronoi faces is slightly smaller than in the polyhedral mesh and the number of Voronoi cells is less than the polyhedral cells. It is worth to mention that this Voronoi meshes are not constrained to the boundary of the domain. Constrained Voronoi meshes require additional vertices and faces to fit the domain geometry.



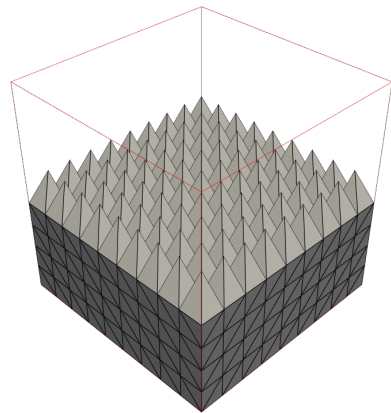
(a) Random mesh



(b) Poisson mesh



(c) Quality mesh



(d) Grid mesh

Figure 5: Example of the meshes generated for the experiments, all meshes have near 5000 vertices. The cubes were cut by a plane to show the interior of the mesh.

	Tetrahedral mesh				Polyhedral mesh							
	#V	#F	#T	#E	#P'	#B. faces	#P. w'barriers	#PolyTetras	Max tetras	Avg tetras	#F'	Time
Random	496	5155	2462	3188	748	477	182	191	15	3.0	3442	0.1
	989	10283	4910	6361	1444	885	369	344	19	3.0	6817	0.3
	4997	59369	29025	35340	8637	5537	2143	2153	21	3.0	38989	1.7
	9988	118495	57917	70565	17032	11019	4265	4164	24	3.0	77617	3.3
	49999	642745	318552	374191	95933	62262	24113	24203	32	3.0	420174	18.9
Poisson	533	5196	2458	3270	828	352	202	168	11	3.0	3566	0.1
	1002	9714	4589	6126	1505	710	381	355	13	3.0	6630	0.3
	4995	56200	27331	33863	9198	4308	2393	2280	16	3.0	38069	1.8
	10557	119178	58005	71729	19355	9126	4966	4606	16	3.0	80532	3.5
	50149	616412	304756	361804	104452	49083	28055	26313	17	3.0	416146	17.2
Quality	513	4729	2227	3014	748	301	178	155	12	3.0	3250	0.1
	996	9586	4553	6028	1533	641	372	360	17	3.0	6568	0.3
	5030	53568	25986	32611	8655	3413	2210	1932	15	3.0	36239	1.5
	10134	111654	54515	67272	18088	7147	4556	3971	14	3.0	75231	3.2
	50027	578629	285369	343286	94196	37881	24128	20154	18	3.0	387486	16.3
Grid	512	4410	2058	2863	690	33	33	7	5	3.0	3042	0.1
	1000	9234	4374	5859	1460	53	53	14	5	3.0	6320	0.3
	4913	50688	24576	31024	8376	1741	1741	471	5	3.0	34476	1.4
	10648	113778	55566	68859	18565	721	721	224	5	3.0	76771	3.4
	50653	567648	279936	338364	93829	8998	8998	2362	5	3.0	381531	15.7

Table 1: Table of the experiments for in-circle criterion. For an input Tetrahedral mesh, “#V” represents the number of vertices, “#F” is the number of faces, “#T” indicates the number of tetrahedrons, and “#E” signifies the number of edges. For the output mesh, “#P” denotes the total number of polyhedrons, “B. Faces” refers to the count of barrier-faces, “P. with barriers” is the number of polyhedrons containing barrier-faces. “#PolyTetras” represents the number of polyhedrons that are tetrahedrons, “Max tetras” is the maximum number of tetrahedrons in a polyhedron, “Avg tetras” gives the average number of tetrahedrons per polyhedron, and “Time” is the duration in milliseconds that the algorithm takes to execute. The colored numbers are to compare the maximum, in red, and minimum, in blue, value obtained in the experiments of 50k vertices.

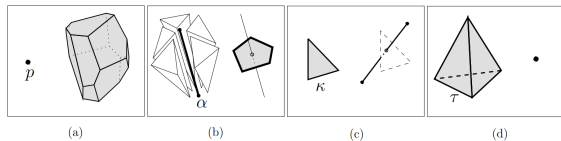


Figure 6: Duality of the 3D Delaunay tetrahedralization DT to Voronoi diagram VD , in (a) each point p of DT is enclosed by a Voronoi cell, in (b) each edge DT has associated a Voronoi face, in (c) each triangle face of DT has associated a Voronoi edge of VD , and in (d) The circumcenter of each tetrahedron circumsphere is a Voronoi point of VD . Source [14].

5 Conclusions and future work

In this paper, we have presented the theoretical concepts and a preliminary version of an algorithm designed to convert a tetrahedral mesh into a polyhedral mesh. We have introduced the concept of terminal/face regions in order to guide the polyhedral construction. The preliminary results show that the algorithm reduces the number of polyhedrons by approximately 70%, and that the average number of tetrahedra per polyhedron is 3.

The algorithm also retains approximately 20% of the tetrahedra in the polyhedral mesh. Those results seem to be almost the same, independent of the chosen joining criterion. This means that the concept of terminal face region as defined in this paper needs to be improved by considering joining strategies that also consider quality criteria of the generated polyhedra. Our ongoing work is taken in consideration the last findings. Moreover we have to test if these polyhedra are useful in the context of VEM simulations.

References

- [1] A. ABDELKADER, C. L. BAJAJ, M. S. EBEIDA, A. H. MAHMOUD, S. A. MITCHELL, J. D. OWENS, AND A. A. RUSHDI, *Vorocrust: Voronoi meshing without clipping*, ACM Trans. Graph., 39 (2020).
- [2] P. ALLIEZ, C. JAMIN, L. RINEAU, S. TAYEB, J. TOURNIS, AND M. YVINEC, *3D mesh generation*, in CGAL User and Reference Manual, CGAL Editorial Board, 5.6.1 ed., 2024.
- [3] R. ALONSO, J. OJEDA, N. HITSCHFELD, C. HERVÍAS, AND L. E. CAMPUSANO, *Delaunay based algorithm for finding polygonal voids in planar point sets*, Astronomy and Computing, 22 (2018), pp. 48–62.

	Tetrahedral mesh				Polyhedral mesh							
	#V	#F	#T	#E	#P'	#B. faces	#P. w'barriers	#PolyTetras	Max tetras	Avg tetras	#F'	Time
Random	496	5155	2462	3188	738	238	146	158	16	3.0	3431	0.0
	989	10283	4910	6361	1448	455	298	265	26	3.0	6821	0.0
	4997	59369	29025	35340	8495	2777	1836	1541	18	3.0	38834	0.2
	9988	118495	57917	70565	16747	5428	3576	3008	22	3.0	77325	0.5
	49999	642745	318552	374191	92339	30704	20275	15856	26	3.0	416526	2.8
Poisson	533	5196	2458	3270	794	178	134	125	12	3.0	3532	0.0
	1002	9714	4589	6126	1394	352	248	210	14	3.0	6520	0.0
	4995	56200	27331	33863	8453	2246	1654	1386	16	3.0	37322	0.2
	10557	119178	58005	71729	18018	4853	3496	2984	23	3.0	79193	0.5
	50149	616412	304756	361804	95469	26172	19457	15573	18	3.0	407135	2.6
Quality	513	4729	2227	3014	711	198	137	129	12	3.0	3213	0.0
	996	9586	4553	6028	1467	372	271	270	13	3.0	6501	0.1
	5030	53568	25986	32611	8234	2177	1591	1426	19	3.0	35817	0.2
	10134	111654	54515	67272	17216	4671	3426	2957	17	3.0	74360	0.5
	50027	578629	285369	343286	89156	24895	18064	14959	19	3.0	382428	3.7
Grid	512	4410	2058	2863	695	311	136	190	16	3.0	3048	0.0
	1000	9234	4374	5859	1301	1086	256	298	15	3.0	6161	0.0
	4913	50688	24576	31024	7127	5386	1615	1464	20	3.0	33248	0.2
	10648	113778	55566	68859	15944	13775	3428	3190	24	3.0	74184	0.8
	50653	567648	279936	338364	78934	68376	17538	14850	24	4.0	366755	2.6

Table 2: Table of the experiments for area criterion. For an input Tetrahedral mesh, “#V” represents the number of vertices, “#F” is the number of faces, “#T” indicates the number of tetrahedrons, and “#E” signifies the number of edges. For the output mesh, “#P” denotes the total number of polyhedrons, “B. Faces” refers to the count of barrier-faces, “P. with barriers” is the number of polyhedrons containing barrier-faces. “#PolyTetras” represents the number of polyhedrons that are tetrahedrons, “Max tetras” is the maximum number of tetrahedrons in a polyhedron, “Avg tetras” gives the average number of tetrahedrons per polyhedron, and “Time” is the duration in milliseconds that the algorithm takes to execute. The colored numbers are to compare the maximum, in red, and minimum, in blue, value obtained in the experiments of 50k vertices.

	In-circle criterion					Area max criterion				
	Random	Poisson	Quality	Grid	Total	Random	Poisson	Quality	Grid	Total
Reduction	70.2%	66.4%	66.6%	66.4%	67.4	70.7%	68.8%	68.3%	70.1%	69.5%
Avg Tetras	3.0	3.0	3.0	3.0	3.0	3.0	3.0	3.0	3.2	3.0
Barriers	25.0%	25.6%	24.9%	8.5%	21.0%	21.1%	18.8%	19.4%	21.1	20.1%
Tetrahedrons	24.8	23.5	22.0	2.3	18.1	18.6	16.0	17.6	21.9	18.5

Table 3: Summary of the results from Tables 1 and 2. The “Reduction” row shows the percentage of tetrahedrons removed by the algorithm. The “Avg tetras” row indicates the average number of tetrahedrons contained within each polyhedron. The “Barrier” row displays the percentage of polyhedrons containing barrier faces. And lastly, the “Tetrahedrons” row presents the total number of tetrahedrons remaining in the mesh. For each row, the colored numbers compare the maximum, in red, and minimum, in blue, value obtained in each distribution experiment.

- [4] M. ATTENE, S. BIASOTTI, S. BERTOLUZZA, D. CABIDDU, M. LIVESU, G. PATANÈ, M. PENNACCHIO, D. PRADA, AND M. SPAGNUOLO, *Benchmark of polygon quality metrics for polytopal element methods*, CoRR, abs/1906.01627 (2019).
- [5] L. BEIRÃO DA VEIGA, C. LOVADINA, AND D. MORA, *A virtual element method for elastic and inelastic problems on polytope meshes*, *Computer Methods in Applied Mechanics and Engineering*, 295 (2015), pp. 327–346.
- [6] M. S. EBEIDA AND S. A. MITCHELL, *Uniform random voronoi meshes*, in *Proceedings of the 20th International Meshing Roundtable, IMR 2011, October 23-26, 2011, Paris, France, 2011*, pp. 273–290.
- [7] P. J. FREY, H. BOROUCHAKI, AND P. L. GEORGE, *Delauany tetrahedralization using an advancing front approach*, in *5th International Meshing Roundtable, 1996*, pp. 31–46.

Delaunay tetrahedral mesh				Voronoi Mesh			Our Polyhedral Mesh		
Vertices	Faces	Tetrahedrons	Edges	Voronoi Cells	Voronoi Faces	Vertices	Vertices	Polyhedra	Faces
513	4729	2227	3014	513	3014	2227	513	748	3250
996	9586	4553	6028	996	6028	4553	996	1533	6568
5030	53568	25986	32611	5030	32611	25986	5030	8655	36239
10134	111654	54515	67272	10134	67272	54515	10134	18088	75231
50027	578629	285369	343286	50027	343286	285369	50027	94196	387486

Table 4: Comparison between the Voronoi mesh and the quality mesh using the in-circle criterion. The table shows the number of vertices, edges, polygons, and faces for each mesh type.

- [8] A. GARGALLO-PEIRÓ, X. ROCA, J. PERAIRE, AND J. SARRATE, *Distortion and quality measures for validating and generating high-order tetrahedral meshes*, Engineering with Computers (Lond.), 31 (2015), pp. 423–437.
- [9] R. V. GARIMELLA, J. KIM, AND M. BERNDT, *Polyhedral mesh generation and optimization for non-manifold domains*, in IMR, 2013, pp. 313–330.
- [10] N. HITSCHFELD, P. CONTI, AND W. FICHTNER, *Mixed Elements Trees: A Generalization of Modified Octrees for the Generation of Meshes for the Simulation of Complex 3-D Semiconductor Devices*, IEEE Trans. on CAD/ICAS, 12 (1993), pp. 1714–1725.
- [11] N. HITSCHFELD-KAHLER, *Generation of 3D mixed element meshes using a flexible refinement approach*, Engineering with Computers, 21 (2005), pp. 101–114.
- [12] Y. HU, Q. ZHOU, X. GAO, A. JACOBSON, D. ZORIN, AND D. PANOZZO, *Tetrahedral meshing in the wild*, ACM Trans. Graph., 37 (2018).
- [13] A. HUSSEIN, F. ALDAKHEEL, B. HUDOBIVNIK, P. WRIGGERS, P.-A. GUIDAULT, AND O. ALLIX, *A computational framework for brittle crack-propagation based on efficient virtual element method*, Finite Elements in Analysis and Design, 159 (2019), pp. 15 – 32.
- [14] H. LEDOUX, *Computing the 3d voronoi diagram robustly: An easy explanation*, in Proceedings of the 4th International Symposium on Voronoi Diagrams in Science and Engineering, ISVD 2007, Pontypridd, Wales, UK, July 9-12, 2007, IEEE Computer Society, 2007, pp. 117–129.
- [15] A. V. LEVITIN, *Introduction to the Design and Analysis of Algorithms*, Addison-Wesley Longman Publishing Co., Inc., USA, 2002.
- [16] S. J. OWEN, *A survey of unstructured mesh generation technology*, in Proceedings of the 7th International Meshing Roundtable, IMR 1998, Dearborn, Michigan, USA, October 26-28, 1998, L. A. Freitag, ed., 1998, pp. 239–267.
- [17] S. PANDAY, C. D. LANGEVIN, R. G. NISWONGER, M. IBARAKI, AND J. D. HUGHES, *Modflow-usg version 1: An unstructured grid version of modflow for simulating groundwater flow and tightly coupled processes using a control volume finite-difference formulation*, Techniques and Methods, (2013).
- [18] N. PIETRONI, M. CAMPEN, A. SHEFFER, G. CHERCHI, D. BOMMES, X. GAO, R. SCATENI, F. LEDOUX, J. REMACLE, AND M. LIVESU, *Hex-mesh generation and processing: A survey*, ACM Trans. Graph., 42 (2023), pp. 16:1–16:44.
- [19] M.-C. RIVARA, *New longest-edge algorithms for the refinement and/or improvement of unstructured triangulations*, International Journal for Numerical Methods in Engineering, 40 (1997), pp. 3313–3324.
- [20] S. SALINAS-FERNÁNDEZ, N. HITSCHFELD-KAHLER, A. ORTIZ-BERNARDIN, AND H. SI, *POLYLLA: polygonal meshing algorithm based on terminal-edge regions*, Engineering with Computers, 38 (2022), pp. 4545–4567.
- [21] W. J. SCHROEDER AND M. S. SHEPHARD, *A Combined Octree/Delaunay Method for fully automatic 3-D Mesh Generation*, International Journal for Numerical Methods in Engineering, 29 (1990), pp. 37–55.
- [22] H. SI, *Tetgen, a delaunay-based quality tetrahedral mesh generator*, ACM Trans. Math. Softw., 41 (2015).
- [23] D. SIEGER, P. ALLIEZ, AND M. BOTSCH, *Optimizing voronoi diagrams for polygonal finite element computations*, in Proceedings of the 19th International Meshing Roundtable, IMR 2010, October 3-6, 2010, Chattanooga, Tennessee, USA, 2010, pp. 335–350.
- [24] T. SORGENTE, S. BIASOTTI, G. MANZINI, AND M. SPAGNUOLO, *Polyhedral mesh quality indicator for the virtual element method*, Computers & Mathematics with Applications, 114 (2022), pp. 151–160.
- [25] ———, *The role of mesh quality and mesh quality indicators in the virtual element method*, Adv. Comput. Math., 48 (2022), p. 3.
- [26] T. SORGENTE, S. BIASOTTI, G. MANZINI, AND M. SPAGNUOLO, *A survey of indicators for mesh quality assessment*, Computer Graphics Forum, 42 (2023), pp. 461–483.
- [27] C. TALISCHI, G. PAULINO, A. PEREIRA, AND I. MENEZES, *Polymesher: A general-purpose mesh generator for polygonal elements written in matlab*, Structural and Multidisciplinary Optimization, 45 (2012), pp. 309–328.
- [28] E. C. V., *Mixed Virtual Element Methods. Applications in Fluid Mechanics.*, B.S. Thesis, Universidad de Concepción, Concepción, Chile, 2015.
- [29] P. WRIGGERS AND B. HUDOBIVNIK, *A low order virtual element formulation for finite elasto-plastic deformations*, Computer Methods in Applied Mechanics,

327 (2017), pp. 459–477.

- [30] P. WRIGGERS, B. D. REDDY, W. T. RUST, AND B. HUDOBIVNIK, *Efficient virtual element formulations for compressible and incompressible finite deformations*, *Computational Mechanics*, 60 (2017), pp. 253–268.
- [31] S. YAMAKAWA AND K. SHIMADA, *Automatic all-hex mesh generation of thin-walled solids via a conformal pyramid-less hex, prism, and tet mixed mesh*, in *IMR*, 2011, pp. 125–141.
- [32] D.-M. YAN, W. WANG, B. LÉVY, AND Y. LIU, *Efficient computation of 3d clipped voronoi diagram*, in *GMP*, 2010, pp. 269–282.
- [33] M. YERRY AND M. SHEPHARD, *Automatic Three-dimensional Mesh Generation by the Modified-Octree Technique*, *International Journal of Numerical Methods in Engineering*, 20 (1984), pp. 1965–1990.